Kinetics of liposome disintegration from foam film studies: Effect of the lipid bilayer phase state [1]

C.S. Vassilieff [a],[*], I. Panaiotov [a], E.D. Manev [a], J.E. Proust [b], Tz. Ivanova [a]

[a] *Biophysical Chemistry Laboratory, Department of Physical Chemistry, Faculty of Chemistry, Sofia University, 1 J. Bourchier ave, 1126 Sofia, Bulgaria*
[b] *Laboratoire de Biophysique, Faculte de Pharmacie, Angers, France*

Abstract

The kinetics of interfacial liposome breakdown is investigated in the thin liquid film microinterferometric set up of Scheludko et al. Suspensions of small unilamellar vesicles of dimyristoylphosphatidylcholine are studied at temperatures above and below the temperature of the main gel–liquid crystal first order phase transition. The experimentally established time traces of the velocity of thinning of foam films are used to estimate the kinetic (rate) constants of interfacial liposome disintegration. New and previously established data for other lipids are summarized and compared with results from kinetic measurements of lipid monolayer formation. The thin film experiments confirm the existence of interfacial liposomal aggregates. A change in the kinetic behaviour is observed, due to the 'melting' of the hydrophobic tails in the lipid aggregates. This may have various consequences of biological and pharmacological importance.

Keywords: Liposomes; Thin liquid film; Marangoni–Gibbs effects; Phase transition temperature

1. Introduction

Lipid molecules are practically insoluble as monomers in water or aqueous electrolyte solutions. At the air–water interface monolayers can be formed either by the classical Langmuir technique (spreading of a lipid solution in a volatile nonpolar solvent) or using an aqueous solution of lipid vesicles (liposomes). Vesicle disintegration should take place to provide lipid monomers of energetically favourable orientation at the air–water interface (see Fig. 1).

The mechanisms and kinetics of transformation of the intact liposomes at the air–water interface are mainly related to short-range hydrophobic molecular interactions and consequently should depend on the phase state of the bilayers. In a bulk solution the first order main phase transition between the ordered gel phase and the less ordered liquid crystalline phase is related to the 'melting' of the lipid hydrophobic tails in the aggregates (see e.g. [1,2]). It affects the equilibrium properties of lipid monolayers and bilayers [3–5]. The increase in the degrees of freedom of lipid structures has various implications of biological and pharmacological interest [6,7].

Here we study the role of main gel–liquid crystal phase transition on the thinning kinetics of foam

---

[*] Corresponding author.
[1] Dedicated to Professor Alexei Scheludko – in memoriam.

films of dimyristoylphosphatidylcholine (DMPC) small unilamellar vesicles solutions. This lipid was chosen because the phase transition temperature, T^*, is close to room temperature ($T^* = 23°C$). The results obtained with the thin liquid films microinterferometric technique are compared to results from transient and equilibrium tensiometry at a single interface [8].

The logic of the paper is based on the simplified kinetic scheme [9–13] depicted in Fig. 1.

At a single interface the experiment begins at zero surface coverage and the kinetics of surface layer formation can be followed by measuring the decrease of the surface tension, σ, expressed as a two-dimensional (2-D) surface pressure π, until an equilibrium or quasi-equilibrium (saturated) surface layer is formed. The simplest case is depicted in Fig. 1a: the unilamellar liposomes disintegrate to form an insoluble monomolecular layer at the interface; per-

fectly it contains only lipid monomers [14–16]. In many cases, however, after an initial disintegration of liposomes surface mesophases (aggregates of unknown exact shape and dimension and polydispersity in both) are being formed in addition to a monomolecular layer [10,11,17–19]. A simplified model is depicted in Fig. 1b; the soluble intact vesicles disintegrate partially covering the surface with insoluble monomers and insoluble aggregates. This first order process is described by a kinetic constant α_{1-2}. The saturated surface layer contains lipid monomers in a thermodynamically stable monomolecular film and thermodynamically metastable aggregates. If this quasi-equilibrium saturated surface layer is perturbed by expansion (as in the thin foam film experiments, described below) the metastable aggregates can act as sources of lipid monomers – the process is described by a kinetic constant α_{2-3}. It is reasonable to expect the process 2–3 to be much faster than the process 1–2. In this study, conditions were found (based on previous experience [9–13]), where the diffusion of intact liposomes does not affect the interfacial kinetics.

In the thin foam film technique the experiment begins with a biconcave drop of liposomal suspension after allowing sufficient time for surface layer formation (saturation). When a foam film is formed, the tangential radial outflow of liquid perturbs the equilibrium distribution of the lipid (surfactant). The perturbation in the surface concentration, $\delta\Gamma$, creates a gradient $d\Gamma/dr$. The gradient in Γ creates a gradient in σ, which governs an effective 'dynamically elastic' behaviour of the fluid surface covered with surfactant molecules. In the case of a completely rigid insoluble monolayer this effect may immobilize tangentially the foam film surfaces. Different compensating surfactant fluxes (surface diffusion, bulk diffusion, sources of surfactant monomers) can lower $d\Gamma/dr$, and hence the gradient in σ, thus leading to a decrease in the 'dynamic elasticity' constant. The latter effects contribute to the increase of the tangential mobility of the film surfaces and hence to an increase in the measurable overall velocity of thinning of the cylindrical thin foam film. The lowest velocity of thinning is obtained with 'rigid' surface layers ensuring the hydrodynamic 'no slip' boundary condition at the film surfaces. This is closely related to many interfacial phenomena known
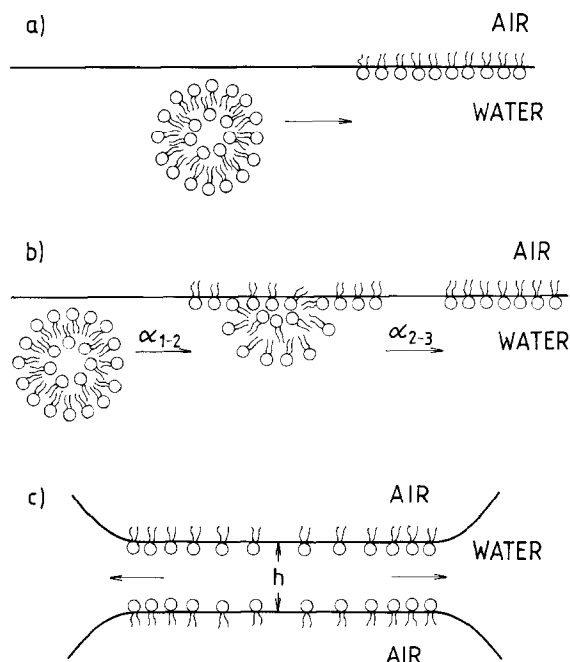

Fig. 1. (a) Intact liposomes disintegrate to form a monomolecular surface lipid layer. (b) Intact liposomes disintegrate partially to form an insoluble monolayer and insoluble surface aggregates (process 1–2). If the surface is perturbed by expansion the metastable aggregates can act as sources of lipid molecules (process 2–3). (c) In the thin liquid film set up the radial flow beneath the surface pertubes the surface layer causing 'dynamically elastic' interfacial effects (see text).

as Marangoni–Gibbs effects (see e.g. the already classical book by Levich [20] and [21]). The experimentally registered rate of thinning of a cylindrical plane-parallel thin foam film, governed by interfacial mass transfer, can be used to find rate determining processes and to estimate interfacial kinetic constants [13,22–27].

2. Materials

2.1. Preparation of liposomes

L-α-Dimyristoylphosphatidylcholine (DMPC) was purchased from Sigma. Analytical grade chloroform from Merck was used. The 0.15 M NaCl solution were made with ultrapure water obtained from a Millipore system and Merck purest quality NaCl heated to 600°C for 90 min.

Small unilamellar liposomes (SUV) were prepared by the Bangham method [28] after sonication above the phase transition temperature $T^* = 23$°C (cell disruptor UZDNA, Russia) for four periods of 15 min interrupted by 5 min resting intervals until the solution became optically almost clear. The liposomal suspensions were filtered through a 0.22 μm Millex GV single-use filter unit (Millipore). The final phospholipid concentration was 10 mg ml^{-1}.

Liposome size measurements were performed with a submicron particle analyser Coulter® Model N4 MD (Coulter Electronics). The mean particle diameter was about 110 nm. The liposome suspensions were stored overnight at $+4$°C and used within 5 days. The change in the size distribution for such a time period is small.

On the assumption that all the phospholipids are contained in spherical unilamellar liposomes with diameter 110 nm, the liposome concentration is $5.7 \cdot 10^{13}$ liposomes per ml.

3. Methods and underlying theory

3.1. Rate of thinning of foam films of DMPC liposomal suspensions

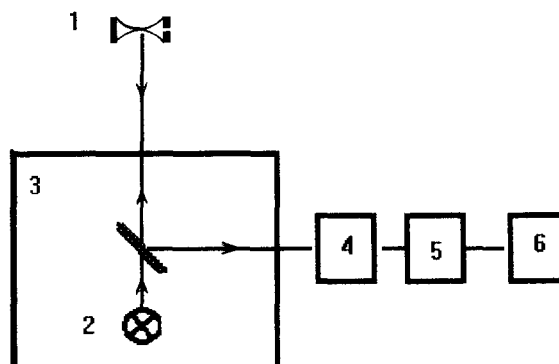The rate of thinning was registered on the microinterferometric set up for studying thin liquid

Fig. 2. Thin liquid films microinterferometric set up: 1, thin foam film in a cut glass capillary holder; 2, light source; 3, metallographic (inverted) microscope; the intensity of the light reflected from the thinning film can be registered: (a) 4, photomultiplier; 5, amplifier; 6, strip-chart recorder and (b) 4, TV-camera; 5, video-recorder; 6, personal computer with image processing hard- and software.

films (see Fig. 2). The established experimental procedure is described in detail elsewhere [29–34]. The registered time trace of the intensity of monochromatic light reflected from the lower and the upper film surfaces (assumed to be plane parallel) is governed by light interference from an optically denser film of diminishing thickness; the interferograms are used to obtain the time trace of the film thickness. The same phenomenon is responsible for the colourful appearance of soap bubbles in polychromatic light.

In the present study the set up was complemented with a thermocouple for direct fine temperature registration in the vicinity of the thermostated film holder and with a TV-video registration, allowing subsequent use of image processing software on a personal computer.

Liposomal suspensions were investigated at temperatures below and above T^* (19 and 26°C).

3.2. Quantification of film thinning data

Under conditions where the film thinning follows a regular pattern and the cylindrical film is almost plane-parallel, the following equations can be used to quantify experimental data.

3.2.1. Film with tangentially immobile surfaces – 'rigid' surface layers [35–37]

$$-(dh/dt)_{Re} = 2h^3(P_c - \Pi)/3\mu R^2 \qquad (1)$$

where t is time, h film thickness, P_c capillary pressure, Π disjoining pressure (in our case Π is the negative attractive van der Waals disjoining pressure, which increases the total film thinning driving pressure, see e.g. [37,38]), μ dynamic viscosity, R radius of a plane-parallel cylindrical film. For the sake of comparison with experimental data it is convenient to express the velocity of thinning dh/dt as $d(h^{-2})/dt = V$. With this notation Eq. 1 can been rewritten as:

$$V_{Re} = 4(P_c - \Pi)/3\mu R^2. \qquad (2)$$

3.2.2. Film with tangentially mobile surfaces – 'dynamically elastic' surface layers

The case of the monomer bulk diffusion controlled process, considered theoretically in [22,26,27], was found also experimentally with solutions of water soluble surfactants (soluble both as monomers and micelles ≡ vesicles) [22,27]. In the present study this case is excluded (water insoluble lipid molecules).

The case of monomer adsorption controlled surface 'dynamic elasticity', considered theoretically in [26], has found its experimental verification with foam films of DPPC liposomal suspensions [13]. In the latter case the 'adsorptive' flux is provided by surface aggregates acting as sources of lipid molecules in the film surface, perturbed by radial liquid flow beneath the surface. The equation for the case of surface sources or monomer adsorption controlled process, derived for small perturbations (linear approximation in the simplest relevant geometry of a cylindrical foam film with plane-parallel surfaces), is sophisticated enough [26]:

$$V/V_{Re} = (3\mu R^2\alpha/4hE_G)[I_0(qR)/I_2(qR)] \qquad (3)$$

where $q^2 = 6\mu\alpha/hE_G(1 + b_s)$, I_0 and I_2 are modified Bessel functions of zeroth and second order, respectively; $b_s = 6\mu D_s/hE_G$; D_s denotes monomer surface diffusivity; $E_G = -(d\sigma/d \ln\Gamma)_0$ is the equilibrium Gibbs' elasticity of the interfacial layer, σ surface tension, Γ surface concentration; the ki-

netic constant α is defined as $j_{ads} = -\alpha \delta\Gamma$, j_{ads} is adsorption flux of surfactant molecules, $\delta\Gamma$ perturbation in the equilibrium surface concentration. According to the simplified kinetic scheme (see Fig. 1b) α should be redefined as α_{1-2} for the slower process 1–2 or as α_{2-3} for the faster process 2–3. The rate constant α_{1-2} describes the disintegration of soluble intact liposomes and α_{2-3} the disintegration of insoluble surface aggregates acting as sources of lipid molecules at the interface, when the equilibrium adsorption layer is disturbed by the tangential flow in the film.

The useful limiting cases of Eq. 3 are:

– at $qR \gg 1$ (negligible surface diffusion) Eq. 3 reduces to

$$V/V_{Re} = 3\mu R^2\alpha/4hE_G \qquad (4)$$

– at $qR \ll 1$ (negligible sources of lipid molecules, surface diffusion being solely responsible for the surface mobility) Eq. 3 reduces to

$$V/V_{Re} = 1 + 6\mu D_s/hE_G. \qquad (5)$$

The latter limiting case was found experimentally with soluble surfactants at very low degrees of surface coverage [24,25].

Our experience has shown that some ambiguities connected with the true exact values of R arise when applying Eqs. 1–5 to treat experimental data [13,39–41]. Hence it is instructive to rewrite Eq. 4 in integral form for higher thicknesses, where $\Pi \ll P_c$ ($h > 60$ nm). Then combining Eqs. 4 and 2 after integration yields (sources of lipid molecules):

$$\Delta(h^{-1})/\Delta t = \alpha P_c/2E_G. \qquad (6)$$

Eq. 2 predicts a decrease in the rate of thinning with increasing the film area (film area $\sim R^2$) due to viscous drag (friction) in the film with 'rigid' surface layers. Eqs. 4 and 5 predict a relative acceleration of the thinning due to the 'dynamic elasticity' of the surface layers. Eq. 4 takes into account only the compensating flux due to surface sources – the 'dynamically elastic' effect is proportional to R^2. Eq. 5 takes into account only the compensating effect of surface diffusion – here the 'dynamically elastic' effect does not depend on film area.

In the integral form of Eq. 6, obtained from Eqs. 2 and 4, the 'viscous' and the 'elastic' effects, both

proportional to R^2, work in opposite directions and $\Delta(h^{-1})/\Delta t$ is insensitive to the film area.

The above predictions are tested experimentally.

4. Results and discussion

It was not an easy task to find conditions (liposome concentrations, film radii and temperatures)

where a regular pattern in the film thinning could be observed and Eqs. 2–6 could be applied for quantification of the experimental results. In the investigated ranges (10 mg/ml down to 0.05 mg/ml; $R \approx 0.01$ cm; 19–23°C) we were not able to register regular film thinning at $T < T^*$ (more than 70 films were observed). At $T > T^*$ we could observe a picture similar to that with soluble surfactants (relatively regular thinning at 130 nm $> h > 60$ nm) at 26°C,
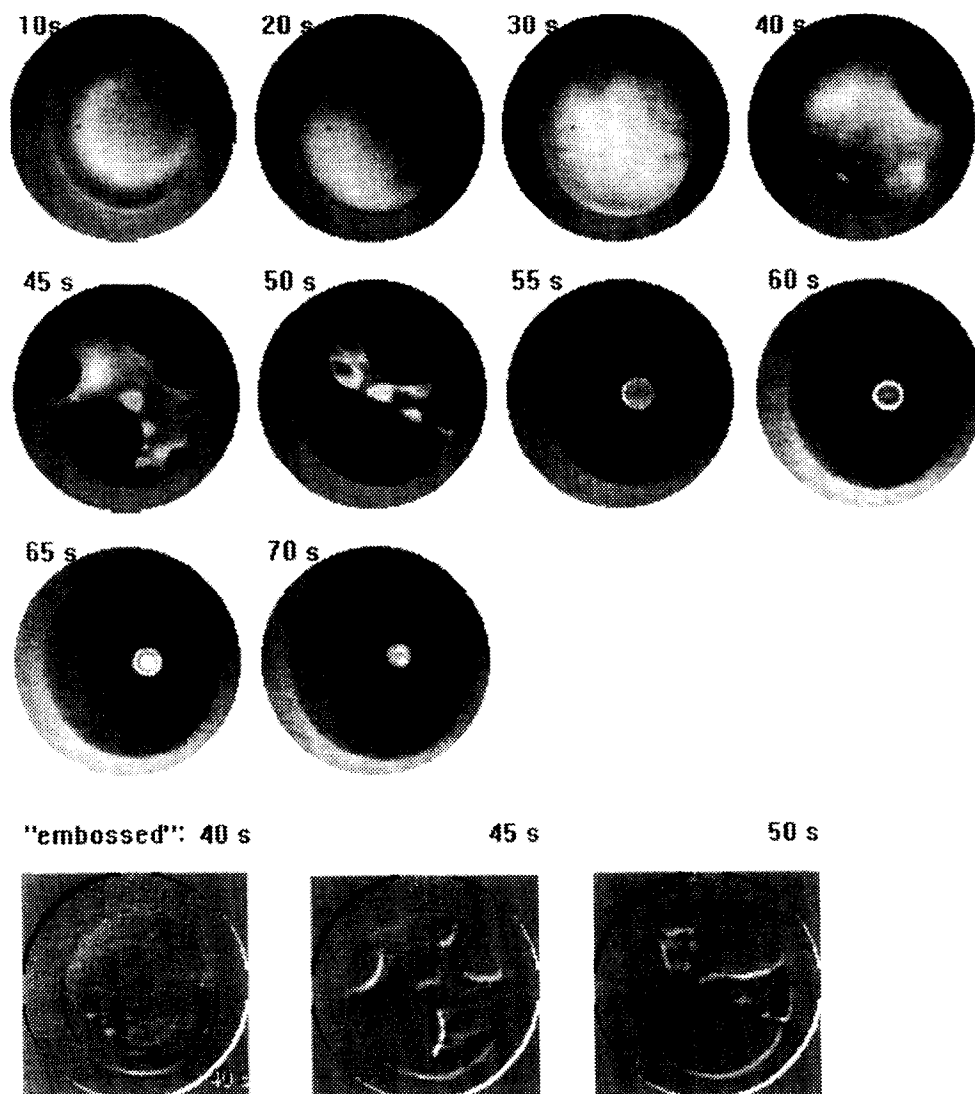

Fig. 3. Chronological sequence of videoframes of a foam film of DMPC liposomal suspension (0.05 mg/ml) at 19°C. Time denoted on the frames is counted from the instant of film formation. The 'embossed' frames exhibit the film shape irregularities after formation of black spots. At $T < T^*$ the significant shape irregularities appearing already at higher thicknesses do not allow to use equations, derived for a plane-parallel film.
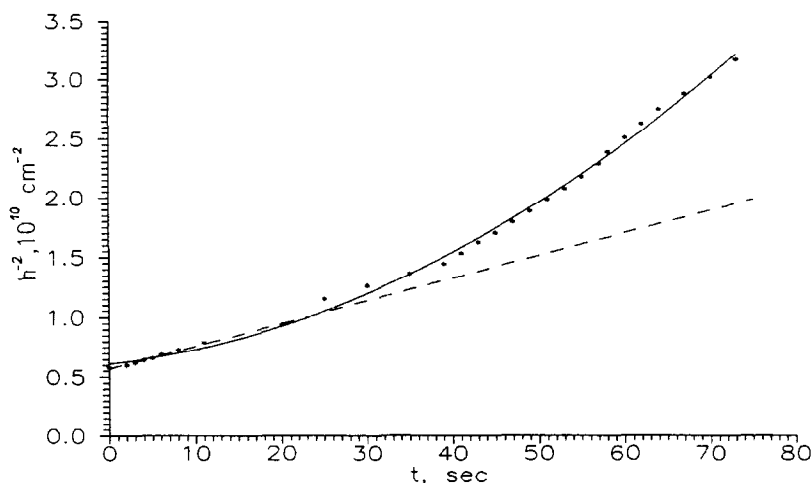
Fig. 4. At $T > T^*$ a relatively regular pattern is observed at $130 < h < 60$ nm, allowing to make use of Eq. 2 to quantify film thinning records; the initial linear slope is used to determine V_x.

bulk liposome concentration of 0.05 mg of lipid per ml 0.15 M aqueous NaCl solution and R in the range of 10^{-2} cm.

The irregular pattern of film thinning at $T < T^*$ (19°C) is depicted as chronological sequence of videoframes in Fig. 3. The interesting new phenomenon of lens formation in a foam liposomal film at $T < T^*$, first reported in [42], is confirmed here. While in the previously reported observation at a higher concentration and same temperature it took minutes for a larger lens to approximate the shape of a two-sided spherical segment, here the thickening of the lens occurs in several seconds,

A set of results at 26°C $(T > T^*)$, where the film thinning behaviour matched approximately model assumptions (cylindrical plane parallel film) in the thickness range 130 nm $> h > 60$ nm, was treated according to Eqs. 2, 4–6.

A typical record of film thinning data is presented in Fig. 4 in the scale suitable to test the predictions of Eq. 2. The predicted trends, confirmed with abundant experimental material collected in the past with soluble surfactants [21,22,24,25,30,31,37,39–41,43], are confirmed in the present case of insoluble lipid molecules (see also [13]). The initial linear slopes (130 nm $> h > 100$ nm) for films with different area are used to obtain an 'experimental' value of V_x. Using these values instead of V_{Re} we tried to overcome ambiguities connected with the quantitative

use of Eq. 2, where the real value of the 'hydrodynamic' film radius is not strictly known[13,37,39–41].

Fig. 5 depicts the linearizing slope of Eqs. 4 and 5. The experimental findings disagree with the predictions of Eq. 5, which does not take into account the presence of sources of lipid molecules on the surface. Rather than being insensitive to film size, as required by Eq. 5, the straight lines in Fig. 5 show the tendency to increase their slopes with film area, as predicted by Eq. 4. Fig. 6 depicts the linearizing
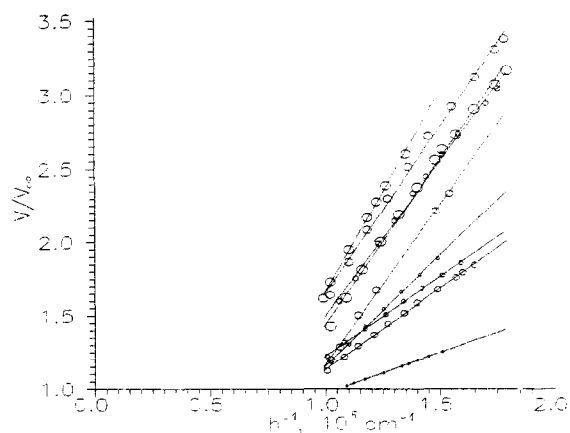

Fig. 5. V / V_x vs. $1/h$ testing the predictions of Eqs. 4 and 5; the slope tends to increase with film area indicated by increasing symbol dimension (26°C, 0.05 mg/ml).
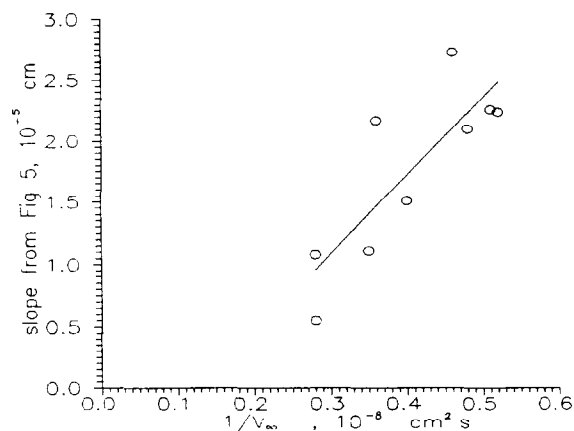
Fig. 6. Slopes from Fig. 5 as a function of $1/V_x \sim R^2$.

Fig. 7. Same film thinning records plotted as a dependence on estimated film area: (a) V_∞ from data at 130 nm $> h >$ 100 nm (cf. Fig. 4); (b) $\Delta h^{-1}/\Delta t$ from data at 100 nm $> h >$ 60 nm, testing the prediction of Eq. 6.

plot, following from Eqs. 2 and 4, of the slopes from Fig. 5 as a function of $1/V_x \sim R^2$. This treatment strongly corroborates the applicability of Eq. 4 to the studied system – the linear dependence of V/V_x on the reciprocal film thickness depicted in Fig. 5 (the intercepts are scattered around zero) and the predicted linear increase the slopes from Fig. 5 on the film area (confirmed in Fig. 6).
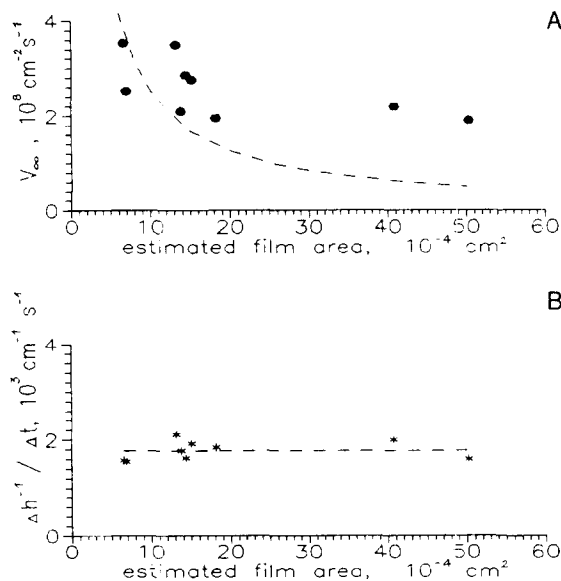
The same conclusion can be drawn when examin-

ing the data presented in Fig. 7 as a function of the estimated film area (from the radius corresponding to the microscopically observed 'first Newton fringe',

Table 1
Kinetic constants [a] of interfacial liposome disintegration (interfacial layer formation)

Lipid	Exp. T (°C)	E_G [b] (mN/m)	α_{1-2} (s^{-1}) (a)	α_{1-2} (s^{-1}) (b)	α_{2-3} (s^{-1}) (c)
DMPC	19	ca. 45 [8]	$6.3 \cdot 10^{-5}$	–	comment [c]
$T^* = 23$°C	21	ca. 45 [8]	$6.3 \cdot 10^{-5}$	–	–
	25	ca. 45 [8]	$1.7 \cdot 10^{-4}$	–	–
	26	–	–	–	10^2
	27	ca. 45 [8]	$1.3 \cdot 10^{-4}$	–	–
DPPC	22	120 [10,11]	$1.2 \cdot 10^{-3}$	$3.6 \cdot 10^{-3}$ [10,11]	10^2 [13]
$T^* = 41$°C		(50) [10,11]		$(3.3 \cdot 10^{-3})$ [10,11]	
DOPC	22	80 [10,11]	$0.5 \cdot 10^{-3}$	$1.5 \cdot 10^{-3}$ [10,11]	comment [c]
$T^* = -22$°C		(50) [10,11]			

[a] DMPC — dimyristoylphosphatidylcholine; DPPC — dipalmitoylphosphatidylcholine; DOPC — dioleylphosphatidylcholine; entries without brackets — from 'spread liposomal suspension' experiments; data in brackets — from 'injected liposomal suspension' experiments (see [10,11]); source of previously reported data is given in square brackets.
[b] Equilibrium dilational Gibbs' elasticity at $\pi = 15$ mN/m from $\pi(A)$ data.
[c] Different qualitative behaviour of foam film thinning depending on phase state (see text).
(a) From transient Langmuir tensiometry (experiment begins at a 'naked' interface): α_{1-2} values estimated from $\Delta\pi(t)$ data with β_{emp} (see Appendix).
(b) From transient interfacial potentiometry (experiment begins at a 'naked' interface): α_{1-2} values estimated from $\Delta V(t)$ data [10,11].
(c) From thin foam films experiments (experiment begins with two 'saturated' interfaces in a biconcave drop — see Fig. 2).

which does not necessarily coincide with the 'hydrodynamic' one):

- Fig. 7a, same film thinning data at 130 nm $> h >$ 100 nm in the form of Eq. 2, c.f. Fig. 4;
- Fig. 7b, same film thinning data at 100 nm $> h >$ 60 nm in the integral form of Eq. 6.

In agreement with the predictions of Eq. 6 the measured ratios of $\Delta(h^{-1})/\Delta t$ are insensitive to the changes in the film radius (and respectively film area), while V_∞ clearly decreases with estimated film area (in overall agreement with the predictions of Eq. 2 presented with the broken line).

The value of the slope in Fig. 6 (c.f. Eq. 4)) is used to estimate the kinetic constant α of release of monomeric lipid material from either intact liposomes (process 1–2) or interfacial aggregates (mesophases, process 2–3); the result is $\alpha/E_G = 11$ (s mN/m)$^{-1}$ (other values used are: $\mu = 1$ mN s/m^2; $P_c = 60$ N/m^2).

The average value $1.77 \cdot 10^3$ (cm s)$^{-1}$ of $\Delta(h^{-1})/\Delta t$ (see Fig. 7b) is also used to estimate the same quantity from Eq. 6 – the result is $\alpha/E_G = 6$ (s mN/m)$^{-1}$, in order of magnitude agreement with the above estimate.

The values of the kinetic constants α are given in Table 1. For comparison previously obtained values for other lipids are also collected in Table 1 and compared with data from transient and equilibrium tensiometry and potentiometry at a single interface [8,10,11] (c.f. Appendix).

Thin foam film experiments give a value of α orders of magnitude higher than experiments at one interface. This indicates that, most probably, the registered acceleration of film thinning is due to the second process 2–3 (see Fig. 1b). Physically it is reasonable to expect the release of monomers from surface aggregates (process 2–3) to be much faster than the actual liposome disintegration (process 1–2), which is responsible for the increase in π detected in experiments beginning at a 'naked' interface. The faster process 2–3 cannot be detected in the latter experiments, because the two processes are in series – the rate of interfacial layer formation is determined by the slower process 1–2. In the thin foam films technique the radial outflow disturbs a layer consisting of a monomolecular layer and surface aggregates. The interfacial coverage perturbation can be compensated either by intact liposome disintegra-

tion (process 1–2) or by monomer release from surface aggregates (process 2–3): the two processes are in parallel and the mass-transfer is determined by the faster process 2–3.

5. Concluding remarks

At a single interface the 'melting' of the hydrophobic tails accelerates liposome interfacial disintegration (surface mesophases formation) [3,8]. The effect is much more pronounced with large (probably multilayer) liposomes [3].

The main gel–liquid crystal phase transition of DMPC is detected also at two hydrodynamically perturbed air–water interfaces (thin foam film). With the thin foam film technique a qualitatively different kinetic behaviour is observed at $T < T^*$: the thinning follows less regular pattern; a tendency of lens formation in foam films is established (see Fig. 3).

Quantitatively (with respect to the kinetic constant α, see Table 1) the expected change with temperature ($T < T^*$ and $T > T^*$) is confirmed with DMPC liposomal suspensions. The thin foam film experiments prove indirectly the existence of interfacial liposomal aggregates ($\alpha_{1-2} \ll \alpha_{2-3}$).

Concurrently, the comparison with the previously established data (see Table 1) indicates that, with respect to α, the lipid individuality may be more important than the phase state.

Acknowledgements

Appendix A. Parametrisation of transient surface pressure data

The nature of surface layers formed from a liposomal suspension, investigated by means of various methods, is still a controversial issue: some researchers claim to find true monomolecular films [14–16], while others find inhomogeneous interfacial

mesophases including bilayers or more complex structures [10,11,17–19]. The formation of a complex surface layer from phosphatidylcholine (PC) liposomes at the air–water interface was first experimentally observed by Verger et al. [44]. Schindler [14] proposed a complex kinetic scheme with five parameters. A simplified kinetic scheme was subsequently developed by Panaiotov et al. [9–12].

The parametrisation of the kinetic curves $\pi(t)$ is based on the simplified scheme depicted in Fig. 1b. The irreversible interfacial transformation of soluble intact liposomes into insoluble surface aggregates and monomers can be described by the Langmuir adsorption kinetic equation without the desorption term [9–12]:

$$\mathrm{d}n^*/\mathrm{d}t = kC_0 d(1 - \theta) \qquad (A1)$$

where n^* is the number of disintegrated intact liposomes per unit area; θ is the relative surface coverage (covered area/total area); d the diameter of an intact liposome; C_0 is the concentration of intact liposomes in the subsurface; $C_0 d$ is the same quantity related to unit area; k is rate constant (of a first kinetic order process at very low surface coverage).

The mass balance relation between n^* and θ depends on model assumptions concerning the structure of the interfacial lipid layer (when, as here, the exact structure and composition of the surface layer is not known).

A.1. Monomolecular insoluble layer

In the simplest situation depicted in Fig. 1a one disintegrating intact liposome, containing N monomers, would cover an area NA_m (A_m denoting the area per molecule in a close-packed monomolecular layer):

$$\theta = n^* NA_m = n^* N/\Gamma_{max} = \Gamma/\Gamma_{max} \qquad (A1i)$$

(Γ is number of monomers per unit area, $\Gamma_{max} = 1/A_m$).

A.2. Monolayer plus one type of surface aggregates

This situation is depicted in Fig. 1b – partial disintegration of one intact liposome would cover an area $(N - N_{agg})A_m + A_{agg}$ (N_{agg} and A_{agg} denoting respectively the number of monomers in the aggre-

gate and the actual area occupied by one aggregate; $n^*_{max} = 1/A_{agg}$ is the maximal number of the aggregates per unit area in a close-packed layer):

$$\theta = n^* \left[\left(N - N_{agg} \right) A_m + A_{agg} \right]$$
$$= n^* \left[\left(N - N_{agg} \right) + A_{agg}/A_m \right] /\Gamma_{max}$$
$$= n^* \left[\left(N - N_{agg} \right) A_m/A_{agg} + 1 \right] /n^*_{max}. \qquad (A1ii)$$

A.3. Surface layer consisting only of aggregates

This limiting case is obtained from Eq. (ii) if $(N - N_{agg}) A_m \ll A_{agg}$ yielding

$$\theta = n^*/n^*_{max}. \qquad (A1iii)$$

In the three cases θ is proportional to n^* and Eq. 1 can be rewritten in a form allowing its easy integration (at $t = 0$, $\theta = 0$)

$$\ln(1 - \theta) = -\alpha t \qquad (A2)$$

where

(i) $\alpha = kC_0 dN/\Gamma_{max}$

(ii) $\alpha = kC_0 d\left[\left(N - N_{agg} \right) A_m + A_{agg} \right]$

(iii) $\alpha = kC_0 d/n^*_{max}$

In order to estimate a kinetic constant of interfacial layer formation from Eq. 2 the time trace of the degree of coverage of the surface $\theta(t)$ is needed, while $\pi(t)$ is measured experimentally. One possibility is to use an equation of state from Langmuir–Szyszkowski type (two dimensional ideal lattice mixture), see e.g. [45] (models (i) and (iii) correspond to equally sized occupied and empty sites with different site area, (i) $A_m = 1/\Gamma_{max}$ or (iii) $A_{agg} = 1/n^*_{max}$). Hence

$$\pi = -\beta \ln(1 - \theta) \qquad (A3)$$

where (i) $\beta = \Gamma_{max} k_B T$ or (iii) $\beta = n^*_{max} k_B T$. In the case (ii) one should use a more complicated equation following from the expression for the entropy of random mixing of differently sized species.

Eq. 3 is used as an empirical equation of state (empirical constant β_{emp}) at high surface coverage ($\theta > 0.5$), where for the studied system interlipid interactions and 'surface-pressure dependent alkylchain entropy' [3] can play a significant role. The simple equation of state (A3) turns out to hold
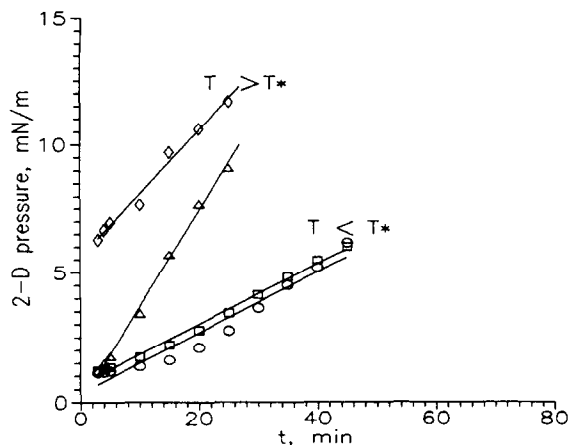
Fig. 8. Transient surface pressure data from [8] at different temperatures treated to obtain linear slopes, predicted by Eq. A4.

reasonably well in the ranges studied in Ref. [8] ($1 < \pi < 12$ mN/m) in the form $\Delta\pi = -\beta\ln(1 - \theta)$. It is used here to convert $\pi(t)$ data into $\theta(t)$ dependence. The combination of Eqs. A2 and A3 yields a simple means to estimate kinetic constants

$$\pi(t) = \alpha\beta t. \qquad (A4)$$

Eq. A4 predicts a linear dependence of $\pi(t)$ on t with a slope $\alpha\beta$; from the experimental slope and an independently measured value of β_{emp} one can determine the value of α.
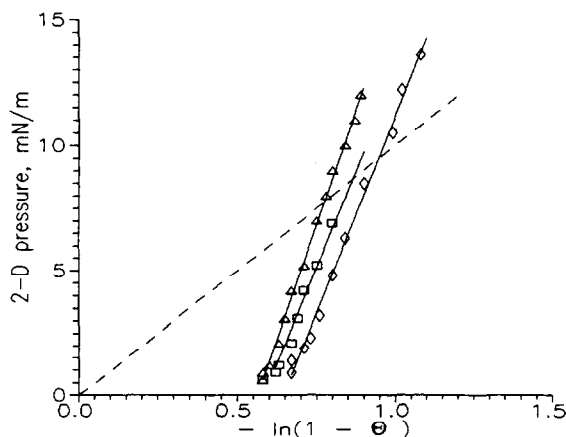

Fig. 9. Surface pressure/area isotherms from [8] at different temperatures treated according to Eq. A3 to obtain β_{emp} (an empirical value of β) for the investigated ranges; the broken line depicts the predictions of Eq. A3 for monomolecular lattice model $\beta = \Gamma_{max} k_B T$.

The procedure is illustrated in Figs. 8 and 9 with experimental data for DMPC from [8]. The slopes ($\Delta\pi/\Delta t$, mN/m s) from linear best fits are: at 19°C, $1.93 \cdot 10^{-3}$; 21°C, $1.95 \cdot 10^{-3}$; 25°C, $6.20 \cdot 10^{-3}$; 27°C, $4.12 \cdot 10^{-3}$. The treatment of equilibrium $\pi(A)$ data from [8] in the scale of Eq. A3, allowing the determination of an empirical constant β_{emp}, is presented in Fig. 9 ($A_m = 44 \cdot 10^{-16}$ cm^2). The values of the slopes (from linear best fit) are close:

19°C $\pi + 18.0 = -30.8\ln(1 - \theta)$

25°C $\pi + 20.1 = -36.6\ln(1 - \theta)$

27°C $\pi + 20.0 = -31.5\ln(1 - \theta)$.

The broken line depicts the predictions of Eq. A3 for a monomolecular film (with (i) $\beta = \Gamma_{max} k_B T$). Obviously the monolayer is not an ideal lattice mixture. But the empirically confirmed linearity in the scale of Fig. 9 allows to make use of the simple form of Eq. A4 and the empirical values of β_{emp} (relevant only for $1 < \pi < 12$ mN/m) to estimate values of the kinetic constant of interfacial layer formation, α. The values are presented in Table 1. They characterize on a relative scale the kinetics of disintegration of SUV from different lipids, but do not reveal the exact (and complex) structure of the interfacial lipid layer.

References

[1] J.F. Holzwarth, in A. Cooper, J.L. Houben and L.C. Chien (Editors), The Enzyme Catalysis Process, Plenum, New York, 1989, p. 383.

[2] Phospholipid phase transitions, Special issue, Chem. Phys. Lipids, 57 (1991) and references therein.

[3] R.C. MacDonald and S.A. Simon, Proc. Natl. Acad. Sci. USA, 84 (1987) 4089.

[4] E. Evans and D. Needham, J. Phys. Chem., 91 (1987) 4219.

[5] D. Exerowa and A. Nikolova, Langmuir, 8 (1992) 3102.

[6] R.E. Pagano and M. Takeichi, J. Cell Biol., 74 (1977) 531.

[7] B. Tenchov, D. Petsev, R. Koynova, C. Vassilieff, H. Mayer and Y. Wunderlich, Colloid Surf., 39 (1989) 361 and references therein.

[8] I. Panaiotov, Tz. Ivanova, K. Balashev and J. Proust, Colloid Surf. A: Physicochem. Eng. Aspects, (1995) in press.

[9] Tz. Ivanova, G. Georgiev, I. Panaiotov, M. Ivanova, M.A. Surpas, J.E. Proust and F. Puisieux, Prog. Colloid Polym. Sci., 79 (1989) 24.

[10] I. Panaiotov and Tz. Ivanova, Commun. Dept. Chem. Bulg. Acad. Sci., 24 (1991) 590.

[11] M.A. Launois-Surpas, Tz. Ivanova, I. Panaiotov, J.E. Proust, F. Puisieux and G. Georgiev, Colloid Polym. Sci., 270 (1992) 901.

[12] Tz. Ivanova, V. Raneva, I. Panaiotov and R. Verger, Colloid Polym. Sci., 271 (1993) 290.

[13] C.S. Vassilieff, I.G. Momtchilova, I. Panaiotov and Tz. Ivanova, Commun. Dept. Chem. Bulg. Acad. Sci., 24 (1991) 519.

[14] H. Schindler, Biochim. Biophys. Acta, 555 (1979) 316.

[15] Th. Schurholz and H. Schindler, Eur. Biophys. J., 20 (1991) 71.

[16] Ch. Salesse, D. Durcharme and R.M. Leblanc, Biophys. J., 52 (1987) 351.

[17] Tz. Ivanova, I. Panaiotov, G. Georgiev, M.A. Surpas, J.E. Proust and F. Puisieux, Colloid Surf., 60 (1991) 263.

[18] O. Belorgey, P. Tchoreloff, J.J. Benattar, J.E. Proust, J. Colloid Interface Sci., 142 (1991) 373.

[19] P. Tchoreloff, A. Gulik, J.E. Proust and F. Puisieux, Chem. Phys. Lipids, 59 (1991) 151.

[20] V.G. Levich, Physicochemical Hydrodynamics, Prentice-Hall, Englewood Cliffs, NJ, 1962.

[21] A. Scheludko, Colloid Chemistry, Elsevier, Amsterdam, 1966.

[22] B. Radoev, E. Manev and I. Ivanov, Kolloid-Z., 234 (1969) 1037.

[23] B.P. Radoev, D.S. Dimitrov and I.B. Ivanov, Colloid Polym. Sci., 252 (1974) 50.

[24] E.D. Manev, C.S. Vassilieff and I.B. Ivanov, Colloid Polym. Sci., 254 (1976) 99.

[25] C.S. Vassilieff, E.D. Manev and I.B. Ivanov, Abhand. Akad. Wiss. DDR, Abtl. Math. Naturwiss. Technik N1 (1986), Akademie Verlag, Berlin, 1987, p. 465.

[26] I.B. Ivanov and D.S. Dimitrov, in I.B. Ivanov (Editor), Thin Liquid Films, M. Dekker, New York, 1988, p. 379.

[27] C.D. Dushkin, C.S. Vassilieff and I.B. Ivanov, Annu. Univ. Sofia, Fac. Chim., 82 (1992) 99.

[28] D. Bangham, M.M. Standish and J.C. Watkins, J. Mol. Biol., 13 (1965) 238.

[29] A. Scheludko, Kolloid-Z., 155 (1957) 39.

[30] A. Scheludko and D. Exerowa, Kolloid-Z., 165 (1959) 148.

[31] A. Scheludko, Adv. Colloid Interface Sci., 1 (1967) 391.

[32] R. Buscall and R.H. Ottewill, in D.H. Everett (Editor), Colloid Science, Specialist periodical reports, vol. 2, The Chemical Society, London, 1975, p. 191.

[33] V.N. Izmailova, G.P. Yampolskaya and B.D. Summ, Surface Phenomena in Protein Systems, Khimia, Moscow, 1988,.

[34] P.M. Kruglyakov and D.R. Excrowa, Foams and Foam Films, Khimia, Moscow, 1990.

[35] O. Reynolds, Phil. Trans. R. Soc. London A, 177 (1886) 157.

[36] A. Scheludko, G. Dessimirov and K. Nikolov, Annu. Univ. Sofia, Fac. Chim., 49 (1954/55) 126.

[37] C. Vassilieff, A. Michailova and E. Basheva, Annu. Univ. Sofia, Fac. Chim., 75 (1981) 184.

[38] S. Nir and C.S. Vassilieff, in I.B. Ivanov (Editor), Thin Liquid Films, M. Dekker, New York, 1988, p. 207.

[39] A. Scheludko and E. Manev, Trans. Faraday Soc., 64 (1968) 1123.

[40] B.P. Radoev, A. Scheludko and E.D. Manev, J. Colloid Interface Sci., 95 (1983) 254.

[41] E.D. Manev, Annu. Univ. Sofia, Fac. Chim., 75 (1981) 74.

[42] C.S. Vassilieff and E.D. Manev, Colloid Polym. Sci., 273 (1995) 512.

[43] E.D. Manev, S.V. Sasdanova, C.S. Vassilieff and I.B. Ivanov, Annu. Univ. Sofia, Fac. Chim., 71 (1976/77) 155.

[44] R. Verger and F. Pattus, Chem. Phys. Lipids, 16 (1976) 285.

[45] T.L. Hill, An Introduction to Statistical Thermodynamics, Addison-Wesley, Reading, MA, 1960.